Phonon linewidths and electron-phonon coupling in graphite and nanotubes

Michele Lazzeri,[1,*] S. Piscanec,[2] Francesco Mauri,[1] A. C. Ferrari,[2,†] and J. Robertson[2]
[1]*Institut de Minéralogie et de Physique des Milieux Condensés, 4 Place Jussieu, 75252, Paris cedex 05, France*
[2]*Cambridge University, Engineering Department, 9 JJ Thompson Avenue, Cambridge CB3 0FA, United Kingdom*
(Received 29 August 2005; revised manuscript received 24 February 2006; published 25 April 2006)

We show that electron-phonon coupling (EPC) is the major source of broadening for the Raman G and G^- peaks in graphite and metallic nanotubes. This allows us to directly measure the optical-phonon EPCs from the G and G^- linewidths. The experimental EPCs compare extremely well with those from the density functional theory. We show that the EPC explains the difference in the Raman spectra of metallic and semiconducting nanotubes and their dependence on tube diameter. We dismiss the common assignment of the G^- peak in metallic nanotubes to a resonance between phonons and plasmons and we attribute it to a resonance between phonons and electron-hole pairs. For metallic tubes, we assign the G^+ and G^- peaks to TO (circumferential) and LO (axial) modes, the opposite of what is commonly done in literature.

DOI: 10.1103/PhysRevB.73.155426 PACS number(s): 73.63.Fg, 63.20.Kr, 73.22.−f

I. INTRODUCTION

Electron-phonon coupling (EPC) is a key physical parameter in nanotubes. Ballistic transport, superconductivity, excited state dynamics, Raman spectra, and phonon dispersions all fundamentally depend on it. In particular, the optical phonons EPC sets the ultimate limit to high field ballistic transport.[1–5] Furthermore, they play a key role in defining the phonon dispersions[6] and the Raman spectra of metallic and semiconducting single wall nanotubes (SWNT).[7–18] Several theoretical and experimental investigations of acoustic phonons EPC have been published (see, e.g., Ref. 19). However, only tight-binding calculations of optical phonons EPC were performed, with contrasting results.[1,2,20–23] More crucially, no direct measurement of optical phonons EPC has been reported.

In this paper we show that the optical phonons EPC is the major source of broadening for the Raman G and G^- peaks in graphite and metallic SWNTs. We show that the experimental Raman linewidths provide a direct EPC measurement. The EPC is also responsible for the the G^+ and G^- splitting in metallic SWNTs. This allows us to assign the G^+ and G^- peaks to TO (circumferential) and LO (axial) modes, in contrast to what is often done in literature.[7,8,10–12,15]

In a perfect crystal, the linewidth γ of a phonon is determined by its interaction with other elementary excitations. Usually, $\gamma=\gamma^{an}+\gamma^{EP}$, where γ^{an} is due to the interaction with other phonons and γ^{EP} with electron-hole pairs. γ^{an} is determined by anharmonic terms in the interatomic potential and is always there. γ^{EP} is determined by the EPC and is present only if the electronic gap is zero. If the anharmonic contribution γ^{an} is negligible or otherwise known, measuring the linewidth is a simple way to determine the EPC.

A phonon is described by a wave vector $\mathbf{q}$, branch index η and pulsation $\omega_{\mathbf{q}\eta}$. We consider a mean-field single particle formalism, such as density functional theory (DFT) or Hartree-Fock. The EPC contribution to $\gamma_{\mathbf{q}\eta}$ is given by the Fermi golden rule:[24]

$$\gamma_{\mathbf{q}\eta}^{EP}=\frac{4\pi}{N_{\mathrm{k}}}\sum_{\mathbf{k},i,j}|g_{(\mathbf{k}+\mathbf{q})j,\mathbf{k}i}|^2[f_{\mathbf{k}i}-f_{(\mathbf{k}+\mathbf{q})j}]\times\delta[\epsilon_{\mathbf{k}i}-\epsilon_{(\mathbf{k}+\mathbf{q})j}+\hbar\omega_{\mathbf{q}\eta}], \quad (1)$$

where the sum is on the electron vectors $\mathbf{k}$ and bands i and j, N_{k} is the number of $\mathbf{k}$ vectors, $f_{\mathbf{k}i}$ is the occupation of the electron state $|\mathbf{k},i\rangle$, with energy $\epsilon_{\mathbf{k}i}$, δ is the Dirac distribution. $g_{(\mathbf{k}+\mathbf{q})j,\mathbf{k}i}=D_{(\mathbf{k}+\mathbf{q})j,\mathbf{k}i}\sqrt{\hbar/(2M\omega_{\mathbf{q}\eta})}$, where M is the atomic mass. $D_{(\mathbf{k}+\mathbf{q})j,\mathbf{k}i}=\langle\mathbf{k}+\mathbf{q},j|\Delta V_{\mathbf{q}\eta}|\mathbf{k},i\rangle$ and $\Delta V_{\mathbf{q}\eta}$ is the potential derivative with respect to the phonon displacement. D is the EPC.

The electron states contributing to the sum in Eq. (1) are selected by the energy conservation condition $\epsilon_{\mathbf{k}i}+\hbar\omega_{\mathbf{q}\eta}=\epsilon_{(\mathbf{k}+\mathbf{q})j}$. Also, the state $\mathbf{k}i$ has to be occupied and $(\mathbf{k}+\mathbf{q})j$ empty, so that the term $[f_{\mathbf{k}i}-f_{(\mathbf{k}+\mathbf{q})j}]\neq 0$. Thus, only electrons in the vicinity of the Fermi level contribute to γ^{EP}. In insulating and semiconducting systems $\gamma^{EP}=0$. In general, a precise estimate of γ^{EP} from Eq. (1) is possible only after an accurate determination of the Fermi surface. However, graphite and SWNTs are very fortunate cases. Thanks to their particular band structure, γ^{EP} is given by a simple analytic formula.

In general, the EPC determines both phonon dispersions and linewidths. We first consider the case of graphite and show that both dispersion and linewidths give a direct measure of the EPC at $\mathbf{\Gamma}$.

II. GRAPHITE

The electron bands of graphite are well described by those of a two-dimensional graphene sheet. In graphene, the gap is zero for the π bands at the two equivalent $\mathbf{K}$ and $\mathbf{K}'=2\mathbf{K}$ points of the Brillouin zone. We define $\langle D_{\mathbf{\Gamma}}^2\rangle_F=\sum_{i,j}^{\pi}|D_{\mathbf{K}i,\mathbf{K}j}|^2/4$, where the sum is on the two degenerate π bands at the Fermi level ϵ_F. We consider the EPC relative to the E_{2g} phonon at $\mathbf{\Gamma}$. The $\mathbf{\Gamma}$-E_{2g} mode is doubly degenerate and consists of an antiphase in-plane motion. For a small $\mathbf{q}$ near $\mathbf{\Gamma}$, this splits into a quasi longitudinal (LO) and quasi

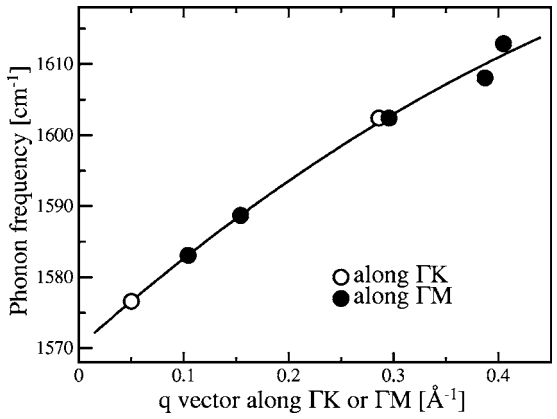

FIG. 1. Graphite phonon dispersion of the highest optical branch near **Γ**. Dots are inelastic x-ray measurements from Ref. 25. The line is a quadratic fit.

transverse (TO) branch, corresponding to an atomic motion parallel and perpendicular to **q**. From DFT calculations we get $\langle D^2_{\mathbf{\Gamma}}\rangle_F$=45.60 (eV/Å)^2 for both LO and TO modes.[6]

A. Phonon frequencies

We have previously shown that graphite has two Kohn anomalies in the phonon dispersions for the **Γ**-E_{2g} and **K**-A_1' modes.[6] Due to the anomaly, the dispersion near **Γ** of the E_{2g}-LO mode is almost linear, with slope $S^{\mathrm{LO}}_{\mathbf{\Gamma}}$:[6]

$$S^{\mathrm{LO}}_{\mathbf{\Gamma}} = \frac{\sqrt{3}\hbar a_0^2}{8M\omega_{\mathbf{\Gamma}}\beta}\langle D^2_{\mathbf{\Gamma}}\rangle_F, \tag{2}$$

where a_0=2.46 Å is the graphite lattice spacing, β=5.52 Å eV is the slope of the electron bands near ϵ_F, M is the carbon atomic mass, and $\omega_{\mathbf{\Gamma}}$ is the pulsation of the E_{2g} phonon ($\hbar\omega_{\mathbf{\Gamma}}$=196.0 meV) (notice that in Ref. 6 the band solpe β=14.1 eV, because the momentum was expressed in units of $2\pi/a_0$). Equation (2) shows that $\langle D^2_{\mathbf{\Gamma}}\rangle_F$ can be directly measured from the experimental $S^{\mathrm{LO}}_{\mathbf{\Gamma}}$. The phonons around **Γ** have been measured by several groups with close agreement. From a quadratic fit to the most recent data of Ref. 25 (Fig. 1) we get $S^{\mathrm{LO}}_{\mathbf{\Gamma}}$=133 cm^{-1} Å. From Eq. (2) we have $\langle D^2_{\mathbf{\Gamma}}\rangle_F$=39 (eV/Å)^2, in good agreement with DFT.

B. Phonon linewidths

We now show that the full width at half maximum of the graphite G peak, FWHM(G), gives another independent EPC measurement. The G peak of graphite is due to the **Γ**-E_{2g} phonon.[26] We use Eq. (1) to compute the width, $\gamma^{EP}_{\mathbf{\Gamma}}$, for this mode. In the vicinity of **K**, the π bands dispersion has a conic shape, with vertex at the Fermi level ϵ_{F} and slope β. For example, the bands at $\mathbf{k}=\mathbf{K}+\mathbf{k}'$, for small $\mathbf{k}'$, are $\epsilon_{(\mathbf{K}+\mathbf{k}')\pi^*}=\beta|\mathbf{k}'|$ and $\epsilon_{(\mathbf{K}+\mathbf{k}')\pi}=-\beta|\mathbf{k}'|$. Thus, for the electronic states that satisfy the energy conservation, $|\mathbf{k}'|=\hbar\omega_{\mathbf{\Gamma}}/(2\beta)$ [Fig. 2(a)]. The E_{2g} is a doubly degenerate mode consisting in an anti-phase movement of the two atoms of the graphene unit cell, along a direction $\hat{\mathbf{r}}$ in the graphene plane. For a small $\mathbf{k}'$, the EPC of the **Γ**-E_{2g} mode is:[6]

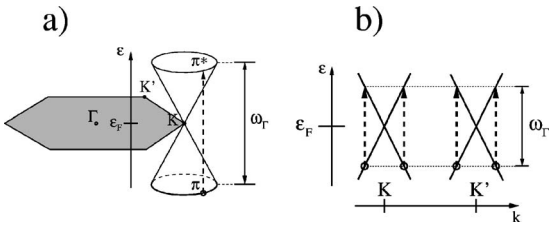

FIG. 2. Electron bands around **K** in graphene (a) and in a metallic tube (b). Shaded area is the graphene Brillouin zone. Dashed arrows: decay processes for a **Γ** phonon.

$$|D_{(\mathbf{K}+\mathbf{k}')\pi^*,(\mathbf{K}+\mathbf{k}')\pi}|^2 = \langle D^2_{\mathbf{\Gamma}}\rangle_F(1+\cos(2\theta)),$$

where θ is the angle between $\mathbf{k}'$ and $\hat{\mathbf{r}}$. For both LO and TO modes:

$$\gamma^{EP}_{\mathbf{\Gamma}} = \frac{\sqrt{3}\hbar a_0^2}{2\pi M\omega_{\mathbf{\Gamma}}}\int d^2k\langle D^2_{\mathbf{\Gamma}}\rangle_F(1+\cos(2\theta))\times\delta(2\beta k-\hbar\omega_{\mathbf{\Gamma}}) = \frac{\sqrt{3}a_0^2\hbar^2}{4M\beta^2}\langle D^2_{\mathbf{\Gamma}}\rangle_F. \tag{3}$$

We used the substitution $1/N_k\Sigma_k=\widetilde{S}/(2\pi)^2\int d^2k$, where $\widetilde{S}=\sqrt{3}/2a_0^2$ is the area of the graphene unit-cell. A factor 2 in Eq. (3) is due to the counting of both **K** and **K**′ Fermi surfaces. Equation (3) gives γ as an energy. Throughout the paper we will express γ as cm^{-1}, the conversion factor is $1/(hc)$, where c is light velocity.

According to Eq. (3), the EPC $\langle D^2_{\mathbf{\Gamma}}\rangle_F$ is directly obtained by measuring the phonon linewidth $\gamma^{EP}_{\mathbf{\Gamma}}$. We then measure FWHM($G$) for a single-crystal graphite similar to that of Ref. 25. Its Raman spectrum does not show any D peak (Reich in Refs. 15 and 27), thus we exclude extra broadening due to disorder.[28] By fitting the G peak with a Lorentzian we get FWHM(G)=13 cm^{-1}. Temperature dependent measurements show no increase of FWHM(G) in the 2–900 K range.[27] Our Raman spectrometer resolution is ~1.5 cm^{-1},[27] thus the experimental intrinsic linewidth is ~13–1.5=11.5 cm^{-1}. By neglecting the anharmonic contribution γ^{an}, we estimate $\gamma^{EP}_{\mathbf{\Gamma}}\sim$11.5 cm^{-1}. Then, from Eq. (3), $\langle D^2_{\mathbf{\Gamma}}\rangle_F\sim$47 (eV/Å)^2. This compares well with DFT, confirming that γ^{an} is small.

Finally, near **Γ** the conservation of the energy and momentum in Eq. (1), implies:

$$\gamma^{EP}_{\mathbf{q}} = 0 \text{ if } q \geqslant \hbar\omega_{\mathbf{\Gamma}}/\beta. \tag{4}$$

Condition (4) is satisfied by the E_{2g} phonon, involved in the Raman G peak. On the other hand, the double resonant mode close to **Γ**, giving the D' peak at ~1615 cm^{-1}, does not satisfy it. D' is indeed sharper than the G peak.[29]

In summary, we presented two independent measurements of the graphite **Γ**-E_{2g} EPC. These are consistent with each other and with DFT. We now consider SWNTs.

III. NANOTUBES

The G peak of SWNTs can be fit with two components,[11] G^+ and G^-. Semiconducting SWNTs have sharp G^+ and G^-,

whilst metallic SWNTs have a broad downshifted G^-.[7–18] The G^- band shows a strong diameter dependence, being lower in frequency for smaller diameters.[11] This suggested its attribution to a circumferential mode, whose atomic displacements would be most affected by a variation in diameter.[10] Thus, the G^+ and G^- peaks are commonly assigned to LO (axial) and TO (circumferential) modes, respectively.[7,8,10–12,15]

Conflicting reports exist on the presence and relative intensity of the G^- band in isolated versus bundled metallic tubes. It has been claimed that this peak is as intense in isolated SWNTs as in bundles;[11,17,18] that it is smaller;[12,14,16] or that it can be absent.[30] The G^- peak is also thought to represent a Fano resonance due to phonon coupling with plasmons.[10,12,13,30,31] Such phonon-plasmon coupling would either need[13] or not need[10,31] a finite phonon wavevector for its activation. The theory of Refs. 10 and 13 predicts the phonon-plasmon peak to be intrinsic in single SWNT, in contrast with 30. On the other hand, the theory in Ref. 13 requires several tubes (>20) in a bundle in order to observe a significant G^- intensity, in contrast with the experimental observation that bundles with very few metallic tubes show a significant G^-.[14,16–18,30] Reference 13 also predicts a G^- upshift with number of tubes in the bundle, in contrast with Ref. 30, which shows a downshift, and with Refs. 10, 11, and 17, which show that the G^- position depends on the tube diameter and not on the bundle size. Finally, the G^- position predicted by 13,31 is at least 200 cm^{-1} lower than that measured.[7–12,14–18] Thus, all the proposed theories for phonon-plasmon coupling[10,13,31] are very qualitative, rely on the guess of several physical quantities, and fail to predict in a precise, quantitative, parameter-free way the observed lineshapes and their dependence on the SWNT diameter.

We now show that, as in graphite, the EPC *per se* gives the main contribution to the G^- position and FWHM in metallic SWNTs, even in the absence of phonon-plasmon coupling. Surprisingly, this has not been considered so far. However, it is clear that, if phonons do not couple to electrons, they certainly cannot couple to plasmons.

A. Phonon frequencies

In a metallic SWNT, the phonon frequencies corresponding to the graphene E_{2g} mode are affected by a Kohn anomaly.[6,32–35] Because of this, in metallic SWNTs the phonon frequencies strongly depend on the electron temperature T_e, as shown in Refs. 33–35. In general, for a smaller T_e, a denser electronic k-point grid is necessary to obtain converged calculations. To compare with measurements done at room conditions, the phonon calculation should be done with $T_e=315$ K and a very dense k-points grid. In Refs. 33 and 34 it has been possible to consider $T_e=315$ K because only small radius tubes ($d\sim0.4$ nm) are considered. On the contrary, in Ref. 32 an unrealistc $T_e=1160$ K has been used in order to reduce the number of k-points required by the calculations. This allowed the treatment of much larger SWNTs (up to $d\sim1.6$ nm). The strength of the Kohn anomaly also depends critically on the quantization of the electronic wave functions along the nanotube circumference (confinement effects). On the contrary, the curvature of the nanotube has a small effect on the strength of the Kohn anomaly. In fact, the curvature can affect the Kohn anomaly by modifying the strength of the EPC and the band dispersion for the states near the Fermi energy. References 3 and 36, respectively, show that, for tube diameters typically used in experiments ($d>0.8$ nm), curvature has a small effect on the EPC and on the band dispersion.

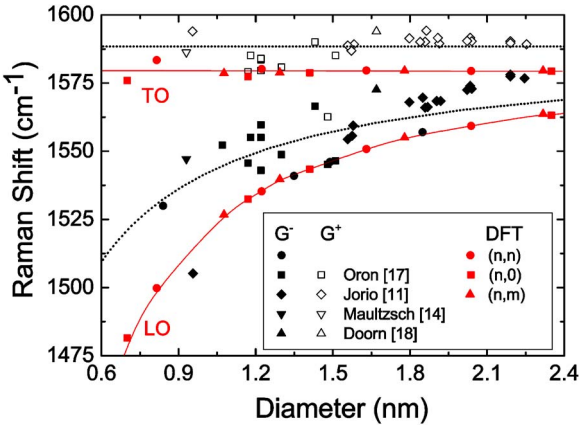

FIG. 3. (Color online) Black points: experimental G^+ and G^- in metallic SWNTs vs diameter. Red points: DFT for armchair [from (6,6) to (15,15)], zigzag [from (9,0) to (30,0)] and chiral tubes [(12,3), (16,1), (16,10), (20,14)]. Lines: fit of Eq. (5) to the experimental and DFT data.

We compute the phonon frequencies for several metallic SWNTs using DFT. For the reasons explained above we neglect the curvature effects but we fully take into account the temperature and the confinement effects. In particular, to simulate a SWNT, we consider planar graphene with two atoms per unit-cell and an interplane spacing of 7 Å. The quantum confinement is fully taken into account by using an appropriate electronic k-point sampling in which only those k-vectors compatible with a given SWNT (see, e.g., Fig. 3 of Ref. 32) are considered. Electrons are occupied with a Fermi-Dirac distribution with $T_e=315$ K for all the tubes. The present approach allows the use of a much more accurate k-points sampling than with the standard methods[32–34] (which require the use of cells with a larger number of atoms). Also, we can treat tubes with any chirality (not only armchair or zig-zag tubes, as in previous works) at a reasonable computational cost. The number of k-points is chosen to have a convergence of the phonon frequencies within 2 cm^{-1}, e.g., for the (11,11) we use 782 points in the graphene unit-cell. DFT calculations are done with the gradient corrected functional of Ref. 37. We use plane-waves (40 Ry cutoff) and pseudopotential approaches.[38] Phonon calculations are done using the perturbative method of Ref. 39.

For all metallic tubes, of any chirality, we get a splitting of the modes corresponding to the graphite Γ-E_{2g} into transverse (TO) and longitudinal (LO), corresponding to atomic motions along the SWNT circumference or parallel to the axis. Thus, the LO/TO classification, which *a priori* is well defined only for achiral tubes and is often considered meaningless in chiral tubes,[40] is on the contrary well-defined for a generic chiral metallic tube.

We find that in metallic tubes the LO frequency is always *smaller* than the TO and has a strong diameter dependence (DFT calculations in Fig. 3). *This is the opposite of what is commonly assumed*, i.e., that a circumferential mode should have a stronger diameter dependence than an axial one.[7,8,10–12,15] This counter-intuitive result is due to the presence of a Kohn anomaly in the phonon dispersion of metallic SWNTs.[6,32,41] The Kohn anomaly lowers the frequency of phonons having significant EPC between electronic states close to the Fermi level (i.e., the EPC which also contributes to the linewidth). While this EPC is large for the LO phonon, the corresponding EPC for the TO is zero. Thus, the LO frequency is smaller than the TO. We thus assign the G^- peak to the LO (axial) mode and the G^+ to the TO (circumferential) mode. In Fig. 3 we compare our calculations with measurements. The agreement between DFT calculations and experiments is excellent. Note that the largest part of the measurements[11,14,17,18] are performed on isolated tubes.

Moreover, since the EPC is inversely proportional to the tube diameter d [this is a simple consequence of Eq. (4) of Ref. 3] it can be proven[41] that:

$$\omega_{LO}^2 = A^2 - B/d; \quad \omega_{TO}^2 = C. \tag{5}$$

with A, B, and C constants. This contrasts with the $1/d^4$ dependence of $\omega_{G^-}^2$ previously suggested.[10,11] Equation (5) is in good agreement with experiments (Fig. 3).

B. Phonon linewidths

Now we use Eq. (1) to derive the EPC contribution to the FWHM of G^+ and G^- in metallic SWNTs, FWHM(G^+), and FWHM(G^-), respectively. The EPC of a SWNT can be obtained from the graphite EPC $\langle D_{\Gamma}^2 \rangle_F$ via zone-folding (valid for $d \geqslant 0.8$ nm, i.e., for SWNTs used in experiments).[3] For energies smaller than 0.5 eV, the electron bands of a SWCN can be approximated linearly as in Fig. 2(b). Because of energy conservation, only π and π^* bands are involved and γ is finite only for phonons with $\mathbf{q} \sim \mathbf{\Gamma}$ or $\mathbf{q} \sim \mathbf{K}$. For $\mathbf{q} \sim \mathbf{\Gamma}$ there are only four electron states giving a finite contribution to γ^{EP} at $\mathbf{k} = \mathbf{K} \pm \hbar\omega_{\mathbf{\Gamma}}/(2\beta)$ and $\mathbf{k} = \mathbf{K}' \pm \hbar\omega_{\mathbf{\Gamma}}/(2\beta)$ [Fig. 2(b)]. The LO and TO linewidths are:

$$\gamma_{\mathbf{\Gamma}-\mathrm{LO}}^{EP} = \frac{2\sqrt{3}\hbar a_0^2}{\pi M \omega_{\mathbf{\Gamma}} \beta} \frac{\langle D_{\mathbf{\Gamma}}^2 \rangle_F}{d}; \quad \gamma_{\mathbf{\Gamma}-\mathrm{TO}}^{EP} = 0. \tag{6}$$

Equation (6) is a key result. It shows that the EPC contributes to the linewidth only for the LO mode in metallic SWNTs. By inserting in Eq. (6) the DFT values, we obtain $\gamma_{\mathbf{\Gamma}-\mathrm{LO}}^{EP} = (79\ \mathrm{cm}^{-1}\ \mathrm{nm})/d$. For semiconducting SWNTs the EPC contribution is zero for both the TO and LO modes, since the energy conservation in Eq. (1) cannot be satisfied because of the electronic gap.

This again confirms our assignment of the G^- and G^+ Raman peaks to the LO and TO modes. Experimentally, in semiconducting SWNTs, FWHM(G^+), and FWHM(G^-) are similar ($\simeq 10\ \mathrm{cm}^{-1}$), while in metallic tubes FWHM(G^-) $\simeq 60\ \mathrm{cm}^{-1}$ and FWHM(G^+) $\simeq 10\ \mathrm{cm}^{-1}$, for a given d.[11,17] The large FWHM(G^-) in metallic SWNTs is due to the large γ^{EP} and the small FWHM(G^+) to other effects.[42] Thus, even if FWHM(G) in graphite and FWHM(G^+) in SWNTs are similar, their origin is different. This also explains why FWHM(G^+) < FWHM(G) can be seen.[11]

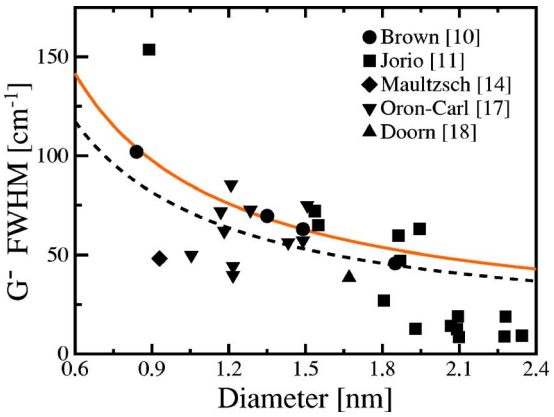

FIG. 4. (Color online) Measured G^- FWHM in metallic SWNTs. Solid line: DFT calculations from Eq. (6) shifted by a constant $\gamma^{an} = 10\ \mathrm{cm}^{-1}$. Dotted line: Fit of FWHM(G^-) $= \gamma_{\mathbf{\Gamma}-\mathrm{LO}}^{EP} + \gamma^{an}$, with $\gamma_{\mathbf{\Gamma}-\mathrm{LO}}^{EP}$ from Eq. (6) and $\gamma^{an} = 10\ \mathrm{cm}^{-1}$.

Equation (6) explains the $1/d$ dependence of FWHM(G^-) in metallic SWNTs.[11] Then, using Eq. (6), $\langle D_{\mathbf{\Gamma}}^2 \rangle_F$ can be directly fit from the experimental FWHM(G^-) (Fig. 4). We find $\langle D_{\mathbf{\Gamma}}^2 \rangle_F = 37\ (\mathrm{eV/\AA})^2$, again in agreement with DFT, given the scattering among experimental data. Note that, while the DFT $\langle D_{\mathbf{\Gamma}}^2 \rangle_F$ is that of planar graphene, the fitted $\langle D_{\mathbf{\Gamma}}^2 \rangle_F$ is obtained from measurements of SWNTs. Thus, the agreement between the two values is a direct verification that the SWNT EPC can be obtained by folding the graphene EPC.[3]

The most common process involved in Raman scattering is single resonance. Double resonance is necessary to explain the activation of otherwise inactive phonons away from $\mathbf{\Gamma}$, such as the D peak.[14,43] It has been suggested that even the G^+ and G^- peaks in SWNTs are always double resonant.[15,44] However, if the laser excitation energy satisfies single resonance conditions, the intensity of single resonance peaks is expected to be dominant in the Raman spectrum.[45] Double resonance can only be relevant for higher excitation energies. The condition set by Eq. (4) must also hold for SWNTs in order to have a significant EPC contribution to the linewidth. Equation (4) can only be satisfied by phonons with wavevector too small to be double resonant.[14,15] Thus, in double resonance, the G^- peak should be much narrower than experimentally observed. Interestingly, it has been reported that the broad G^- peak disappears by increasing the excitation energy while measuring the Raman spectrum of a metallic SWNT, and a sharper one appears (see Fig. 2 of Ref. 14). We explain this as a transition from single to double resonance.

Finally, in Ref. 3 we computed the zero-temperature lifetime τ of a conduction electron in a SWNT, due to phonon scattering. If phonons are thermalized, τ determines the zero temperature electron mean free path $l_0 = \beta\tau/\hbar$. Comparing Eq. (1) here with Eq. (1) of Ref. 3, the linewidths can be expressed as a function of τ as:

$$\gamma_{\mathbf{\Gamma}-LO}^{EP} = 4\hbar/\tau_{\mathbf{\Gamma}-LO}^{bs} = 4\hbar/\tau_{\mathbf{\Gamma}-TO}^{fs} \tag{7}$$

where $bs(fs)$ indicate back (forward)-scattering.[3] Such simple relations might seem surprising. In fact, the two quan-

tities γ^{-1} and τ describe two distinct phenomena: γ^{-1} is the lifetime of a phonon [Eq. (1) here] and τ is the lifetime of an electron [Eq. (1) of Ref. 3]. In general, one does not expect a simple relation between γ^{-1} and τ. However, due to the low dimensionality, in SWNTs γ^{EP} determines directly τ [Eq. (7)]. Thus, the measured γ^{EP} are also a direct measurement of l_0 for metallic SWNTs. Since the measured γ^{EP} is in agreement with DFT calculations, the results of Ref. 3 are further confirmed.

Notice that the lifetime of a phonon coupled with a continuum of excitations [as the one given by Eq. (1)] is an intrinsic property of the system, independent of the experimental probe. Instead, the shape of a peak observed in an actual experiment depends on the coupling of the experimental probe with the system, as discussed in the seminal paper by Fano.[46] Indeed, if the probing laser is coupled not only with the phonon, but also with the continuum which broadens the phonon, the Raman spectrum shows an asymmetric Fano profile.[46] Thus, the detection of an asymmetric Fano profile in a Raman measurement gives information on how the electro-magnetic radiation couples to the system, *but not* on the origin of the broadening. Here, we show that the broadening of the G^- peak in metallic nanotubes is due to the coupling of the LO (axial) phonon with the continuum of the electron-hole excitations and not with a plasmon. This does not imply that a Fano-like profile cannot be observed in experiments, but just that the assignement of this profile to phonon-plasmon coupling is incorrect.

IV. CONCLUSIONS

In conclusion, we presented a set of simple formulas [Eqs. (2), (3), and (6)], with the graphite EPC as the *only* fit parameter. Remarkably, these formulas *quantitatively* explain a string of experiments, ranging from phonon slopes and G peak FWHM in graphite to G^- peak position and G^- FWHM diameter dependence in SWNTs. Fitting a wide set of independent data we obtain the *same* EPCs ±10%. These experimental EPC are in excellent agreement with, and validate, the DFT approach. This allows us to propose an interpretation for the Raman spectra of metallic nanotubes. We dismiss the common assignment of the G^- peak in metallic nanotubes to a resonance between phonons and plasmons and we attribute it to a resonance between phonons and electron-hole pairs. For metallic tubes, we assign the G^+ and G^- peaks to TO (circumferential) and LO (axial) modes, the opposite of what is commonly done.

ACKNOWLEDGMENTS

Calculations were performed at HPCF (Cambridge) and IDRIS (Project No. 051202) using the quantum-espresso package (http://www.pwscf.org). We acknowledge S. Reich and C. Thomsen for providing single crystal graphite, and M. Oron-Carl and R. Krupke for useful discussions. S.P. acknowledges funding from IHP-HPMT-CT-2000-00209 and CANAPE. A.C.F. acknowledges funding from The Royal Society and EPSRC Grant No. GR/S97613.

*Electronic address: lazzeri@impmc.jussieu.fr
†Electronic address: acf26@eng.cam.ac.uk

[1] Z. Yao, C. L. Kane, and C. Dekker, Phys. Rev. Lett. **84**, 2941 (2000).
[2] J. Y. Park, S. Rosenblatt, Y. Yaish, V. Sazonova, H. Üstünel, S. Braig, T. A. Arias, P. W. Brouwer, and P. L. McEuen, Nano Lett. **4**, 517 (2004).
[3] M. Lazzeri, S. Piscanec, F. Mauri, A. C. Ferrari, and J. Robertson, Phys. Rev. Lett. **95**, 236802 (2005).
[4] V. Perebeinos, J. Tersoff, and P. Avouris, Phys. Rev. Lett. **94**, 086802 (2005).
[5] A. Javey, J. Guo, M. Paulsson, Q. Wang, D. Mann, M. Lundstrom, and H. Dai, Phys. Rev. Lett. **92**, 106804 (2004).
[6] S. Piscanec, M. Lazzeri, F. Mauri, A. C. Ferrari, and J. Robertson, Phys. Rev. Lett. **93**, 185503 (2004).
[7] M. A. Pimenta, A. Marucci, S. A. Empedocles, M. G. Bawendi, E. B. Hanlon, A. M. Rao, P. C. Eklund, R. E. Smalley, G. Dresselhaus, and M. S. Dresselhaus, Phys. Rev. B **58**, R16016 (1998).
[8] H. Kataura, Y. Kumazawa, Y. Maniwa, I. Umezu, S. Suzuki, Y. Ohtsuka, and Y. Achiba, Synth. Met. **103**, 2555 (1999).
[9] P. M. Rafailov, H. Jantoljak, and C. Thomsen, Phys. Rev. B **61**, 16179 (2000).
[10] S. D. M. Brown, A. Jorio, P. Corio, M. S. Dresselhaus, G. Dresselhaus, R. Saito, and K. Kneipp, Phys. Rev. B **63**, 155414 (2001).
[11] A. Jorio, A. G. Souza Filho, G. Dresselhaus, M. S. Dresselhaus, A. K. Swan, M. S. Ünlü, B. B. Goldberg, M. A. Pimenta, J. H. Hafner, C. M. Lieber, and R. Saito, Phys. Rev. B **65**, 155412 (2002); A. Jorio, C. Fantini, M. S. S. Dantas, M. A. Pimenta, A. G. Souza Filho, G. G. Samsonidze, V. W. Brar, G. Dresselhaus, M. S. Dresselhaus, A. K. Swan, M. S. Ünlü, B. B. Goldberg, and R. Saito, *ibid.* **66**, 115411 (2002); M. S. Dresselhaus, A. Jorio, A. G. Souza Filho, G. Dresselhaus, and R. Saito, Physica B **323**, 15 (2002).
[12] C. Jiang, K. Kempa, J. Zhao, U. Schlecht, U. Kolb, T. Basche, M. Burghard, and A. Mews, Phys. Rev. B **66**, 161404(R) (2002).
[13] K. Kempa, Phys. Rev. B **66**, 195406 (2002).
[14] J. Maultzsch, S. Reich, U. Schlecht, and C. Thomsen, Phys. Rev. Lett. **91**, 087402 (2003).
[15] Papers of a theme issue, edited by A. C. Ferrari and J. Robertson: A. Jorio, R. Saito, G. Dresselhaus, and M. S. Dresselhaus, Philos. Trans. R. Soc. London, Ser. A **362**, 2311 (2004); C. Thomsen, S. Reich, and J. Maultzsch, *ibid.* **362**, 2337 (2004); S. Reich and C. Thomsen, *ibid.* **362**, 2269 (2004); P. Tan, S. Dimovski, and Y. Gogotsi, *ibid.* **362**, 2289 (2004).
[16] H. Telg, J. Maultzsch, S. Reich, and C. Thomsen, *Proceedings of IWEPNM 2005* (AIP, Melville, NY, 2005).
[17] M. Oron-Carl, F. Hennrich, M. M. Kappes, H. v. Lohneysen, and R. Krupke, Nano Lett. **5**, 1761 (2005).
[18] S. K. Doorn, M. J. O'Connell, L. Zheng, Y. T. Zhu, S. Huang, and J. Liu, Phys. Rev. Lett. **94**, 016802 (2005).
[19] T. Hertel and G. Moos, Phys. Rev. Lett. **84**, 5002 (2000).
[20] J. Jiang, R. Saito, A. Gruneis, G. Dresselhaus, and M. S. Dressel-

haus, Chem. Phys. Lett. **392**, 383 (2004).
[21] G. D. Mahan, Phys. Rev. B **68**, 125409 (2003).
[22] G. Pennington and N. Goldsman, Phys. Rev. B **68**, 045426 (2003).
[23] J. Jiang, R. Saito, A. Grüneis, S. G. Chou, G. G. Samsonidze, A. Jorio, G. Dresselhaus, and M. S. Dresselhaus, Phys. Rev. B **71**, 045417 (2005).
[24] P. B. Allen, Phys. Rev. B **6**, 2577 (1972); P. B. Allen and R. Silberglitt, *ibid.* **9**, 4733 (1974).
[25] J. Maultzsch, S. Reich, C. Thomsen, H. Requardt, and P. Ordejón, Phys. Rev. Lett. **92**, 075501 (2004).
[26] F. Tuinstra and J. Koenig, J. Chem. Phys. **53**, 1126 (1970).
[27] V. Scardaci and A. C. Ferrari (unpublished).
[28] A. C. Ferrari and J. Robertson, Phys. Rev. B **61**, 14095 (2000); **64**, 075414 (2001).
[29] P. H. Tan, C. Y. Hu, J. Dong, W. Shen, and B. Zhang, Phys. Rev. B **64**, 214301 (2001).
[30] M. Paillet, P. Poncharal, A. Zahab, J. L. Sauvajol, J. C. Meyer, and S. Roth, Appl. Phys. Lett. **94**, 237401 (2005).
[31] S. M. Bose, S. Gayen, and S. N. Behera, cond-mat/0506004 (unpublished) .
[32] O. Dubay, G. Kresse, and H. Kuzmany, Phys. Rev. Lett. **88**, 235506 (2002); O. Dubay and G. Kresse, Phys. Rev. B **67**, 035401 (2003).
[33] K.-P. Bohnen, R. Heid, H. J. Liu, and C. T. Chan, Phys. Rev. Lett. **93**, 245501 (2004).
[34] D. Connétable, G.-M. Rignanese, J.-C. Charlier, and X. Blase, Phys. Rev. Lett. **94**, 015503 (2005).
[35] R. Barnett, E. Demler, and E. Kaxiras, Phys. Rev. B **71**, 035429 (2005).
[36] V. Zólyomi and J. Kürti, Phys. Rev. B **70**, 085403 (2004).
[37] J. P. Perdew, K. Burke, and M. Ernzerhof, Phys. Rev. Lett. **77**, 3865 (1996).
[38] N. Troullier and J. L. Martins, Phys. Rev. B **43**, 1993 (1991).
[39] S. Baroni, S. de Gironcoli, A. Dal Corso, and P. Giannozzi, Rev. Mod. Phys. **73**, 515 (2001).
[40] S. Reich, C. Thomsen, and P. Ordejon, Phys. Rev. B **64**, 195416 (2001).
[41] S. Piscanec *et al.* (unpublished).
[42] E.g., anharmonicity, inhomogeneous broadening and coupling with a substrate. FWHM(G^-) and FWHM(G^+) increase $\sim 15\ \mathrm{cm}^{-1}$ with temperature in the 80–600 K range for both metallic and semiconducting SWNTs (Refs. 11 and 27). Thus $\gamma^{an} \ll \gamma^{EP}$.
[43] C. Thomsen and S. Reich, Phys. Rev. Lett. **85**, 5214 (2000).
[44] J. Maultzsch, S. Reich, and C. Thomsen, Phys. Rev. B **65**, 233402 (2002).
[45] M. A. Pimenta *et al.*, in *Proceedings of IWEPNM 2003* (AIP, Melville, NY, 2003).
[46] U. Fano, Phys. Rev. **124**, 1866 (1961).